

# Local gene knockdown in the brain using viral-mediated RNA interference

Jonathan D Hommel, Robert M Sears, Dan Georgescu, Diana L Simmons & Ralph J DiLeone

**Conditional mutant techniques that allow spatial and temporal control over gene expression can be used to create mice with restricted genetic modifications. These mice serve as powerful disease models in which gene function in adult tissues can be specifically dissected. Current strategies for conditional genetic manipulation are inefficient, however, and often lack sufficient spatial control. Here we use viral-mediated RNA interference (RNAi) to generate a specific knockdown of *Th*, the gene encoding the dopamine synthesis enzyme tyrosine hydroxylase, within midbrain neurons of adult mice. This localized gene knockdown resulted in behavioral changes, including a motor performance deficit and reduced response to a psychostimulant. These results underscore the potential of using viral-mediated RNAi for the rapid production and testing of new genetic disease models. Similar strategies may be used in other model species, and may ultimately find applications in human gene therapy.**

Animal models are essential for uncovering the molecular mechanisms of disease, but the use of transgenic and knockout mice is limited by developmental effects, genetic compensation and lack of regional specificity. Genetic analysis of the mammalian brain poses a particular challenge, as many genes are broadly expressed and are likely to function in multiple neuronal circuits. The development of efficient techniques and strategies for the generation of conditional mutants is essential for gaining a better understanding of gene function in the context of neuroanatomy.

Current approaches for generating conditional mutants depend on the production of transgenic mice expressing recombinase proteins in restricted regions<sup>1,2</sup>. The isolation of specific regulatory elements can be challenging<sup>3</sup>, however, and transgene insertion sites often influence patterns of expression. It has thus been difficult to systematically generate transgenic lines expressing recombinase proteins in specified brain regions. We therefore sought to develop an efficient strategy for modifying gene function in defined regions of the adult brain.

The discovery of RNAi has revolutionized genetic studies in *Drosophila*, *Caenorhabditis elegans* and mammalian cell culture. By expressing double-stranded RNA, gene knockdowns can be efficiently generated<sup>4</sup>, allowing large-scale screens for gene function to

be conducted<sup>5,6</sup>. Restricted expression of double-stranded RNA has been used to generate conditional gene knockdowns in *Drosophila*<sup>7,8</sup>, while small interfering RNA (siRNA) and short hairpin RNA (shRNA) have proven effective in reducing gene expression in cultured mammalian cells<sup>9–11</sup>. RNAi has also been used to knock down gene expression in the mouse liver<sup>12,13</sup>, and evidence exists for the knockdown of reporter genes in the mouse brain<sup>13</sup>.

We sought to develop a strategy for removing endogenous genes from specific neural circuits of the brain, allowing for the development of more refined disease models. Because adeno-associated virus (AAV) is known to maintain gene expression for long periods<sup>14</sup> and to infect neurons efficiently<sup>15</sup>, we used it as the vector for delivery and expression of shRNA. Using AAV, we targeted tyrosine hydroxylase mRNA within neurons of the midbrain<sup>16,17</sup>. Tyrosine hydroxylase is a key enzyme for the production of dopamine, a neurotransmitter important in a wide range of behaviors, including food intake, addiction, and control of movement<sup>18–20</sup>. Moreover, the degeneration of dopaminergic neurons in the midbrain substantia nigra compacta is the primary cause of Parkinson disease<sup>21</sup>. By targeting specific sets of dopamine neurons, we demonstrate the efficiency of viral-mediated RNAi in reducing gene expression, and its potential for generating models of disease.

## RESULTS

### Viral-mediated knockdown of *Th*

An AAV vector (Fig. 1a) was designed to express both enhanced green fluorescent protein (EGFP), allowing for detection of infected neurons, and a U6 promoter-driven shRNA<sup>10</sup>. We generated two viruses expressing shRNAs (AAV-shTH1 and AAV-shTH2), each of which targets a distinct sequence of *Th*, as well as a control virus with a scrambled sequence (AAV-shSCR). Stereotaxic injections were used to deliver the AAV-shTH1 virus into one side, and AAV-shSCR into the other side, of the substantia nigra compacta of 9-week-old C57BL/6J mice. After 12 d, mice were evaluated for expression of EGFP and tyrosine hydroxylase by double immunofluorescence. We observed a substantial reduction in tyrosine hydroxylase staining in AAV-shTH1-infected cells of the substantia nigra compacta, whereas cells infected with control virus showed normal tyrosine hydroxylase expression

Department of Psychiatry, The University of Texas Southwestern Medical Center at Dallas, 5323 Harry Hines Blvd., Dallas, Texas 75390–9070, USA. Correspondence should be addressed to R.J.D. (ralph.dileone@utsouthwestern.edu)

Published online 23 November 2003; doi:10.1038/nm964

(Fig. 1b–g). Similar results were seen in experiments using AAV-shTH2 in conjunction with two independent negative control viruses (data not shown), confirming that the shRNAs were specific. The remaining experiments used the AAV-shTH1 virus (hereafter referred to as AAV-shTH). These data indicate that AAV-mediated RNAi efficiently reduces endogenous gene expression in midbrain dopamine neurons.

**Time-course analysis of *Th* knockdown**

To assess the dynamics of RNAi-mediated tyrosine hydroxylase reduction in detail, we monitored tyrosine hydroxylase levels between days 6 and 19 after injection, by directly counting the number of infected dopamine neurons with undetectable levels of tyrosine hydroxylase. To count neurons, we used triple immunostaining for EGFP, tyrosine hydroxylase and dopa-decarboxylase (DDC), a marker for dopamine neurons that is normally coexpressed in >95% of tyrosine hydroxylase neurons in the mouse midbrain (data not shown). At early time points, we observed coexpression of all three markers, indicating normal tyrosine hydroxylase levels in infected neurons (Fig. 2a,b). This is consistent with the onset of detectable AAV-mediated expression (days 4–6) and the estimated *in vivo* half-life (~72 h) of tyrosine hydroxylase<sup>22</sup>. By day 12, however, we observed a marked decrease in tyrosine hydroxylase expression in cells expressing both EGFP and DDC, whereas control neurons infected with AAV-shSCR main-

tained high levels of tyrosine hydroxylase at all time points analyzed (Fig. 2a,b). Quantitative analysis at day 19 showed a further reduction in the number of infected, DDC-expressing neurons that also expressed tyrosine hydroxylase (Fig. 2b). Finally, mice analyzed 50 d after viral infection showed persistent EGFP expression and *Th* knockdown (Supplementary Fig. 1 online).

**Quantitation of *in vivo Th* knockdown**

We used quantitative RT-PCR to analyze RNA extracted from cells of the ventral tegmental area (VTA), a dense region of midbrain dopamine neurons. We used laser-capture microscopy to remove AAV-shTH-infected VTA cells, which were identified for removal by detection of EGFP. Real-time RT-PCR analysis revealed a substantial decrease in tyrosine hydroxylase mRNA in neurons infected with AAV-shTH, compared with neurons infected with control AAV-shSCR vector (Fig. 2c). We also assessed changes in expression of DDC, dopamine D2 receptor (D2-R) and vacuolar ATPase. DDC mRNA was modestly downregulated, whereas D2-R and vacuolar ATPase levels were unchanged in the *Th* knockdown neuron clusters (Fig. 2c). However, DDC regulation was an order of magnitude less than the knockdown of *Th*, and may reflect cellular adjustments of DDC mRNA levels in response to the loss of tyrosine hydroxylase function.

**Effects of *Th* knockdown on overall tyrosine hydroxylase production**

Injections into the midbrain showed an ~800- $\mu$ m anterior-posterior spread of the virus, 2 weeks after infection. This resulted in marked infection in a large portion of the substantia nigra compacta (Fig. 3a). We also evaluated knockdown throughout the entire VTA by measuring the overall decrease in tyrosine hydroxylase mRNA. Laser microdissection was used to remove the VTA regions infected with either AAV-shTH or AAV-shSCR. We sampled six sections, spaced ~150  $\mu$ m apart, covering the anterior to the posterior extent of the VTA. Using real-time RT-PCR analysis, we detected a 36% decrease in tyrosine hydroxylase mRNA throughout the AAV-shTH-infected VTA (Fig. 3b).

Because tyrosine hydroxylase regulates dopamine production in synaptic terminals, we assessed the consequences of midbrain AAV-shTH infection on tyrosine hydroxylase levels in the forebrain. First, stereotaxic injections were used to deliver AAV-shTH into one side, and AAV-shSCR into the other side, of the VTA of 9-week-old C57BL/6J mice. Two weeks later, the nucleus accumbens (a forebrain target of VTA dopamine neurons) was removed from either side and evaluated for tyrosine hydroxylase levels. A significant ( $P < 0.05$ ) reduction (~30%) in tyrosine hydroxylase was seen on the AAV-shTH-infected side, compared with the AAV-shSCR-infected side (Fig. 4a,b). We took advantage of our EGFP label to distinguish regions of the nucleus accumbens that were innervated

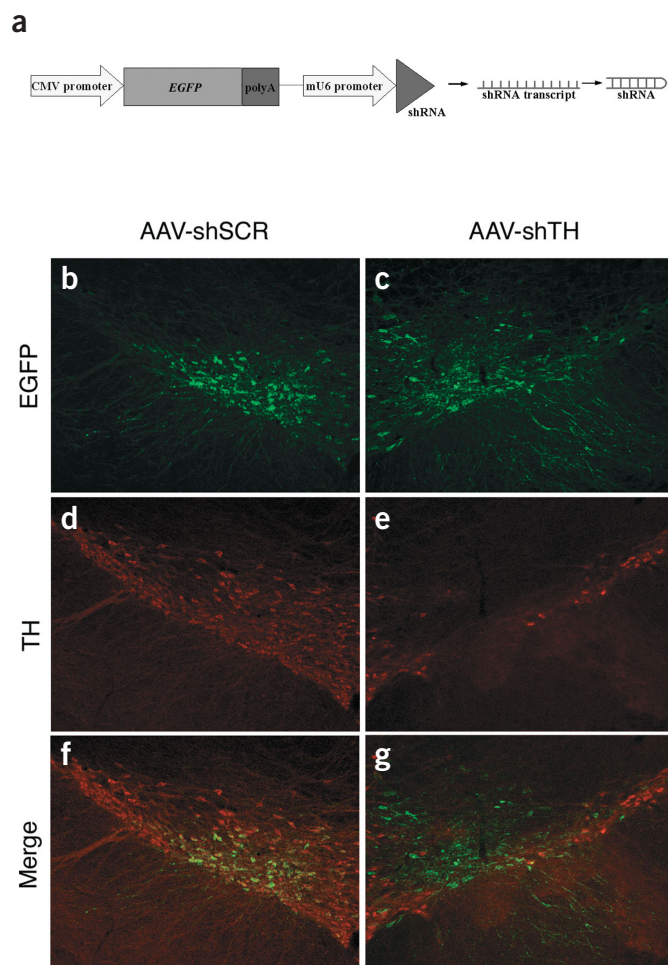
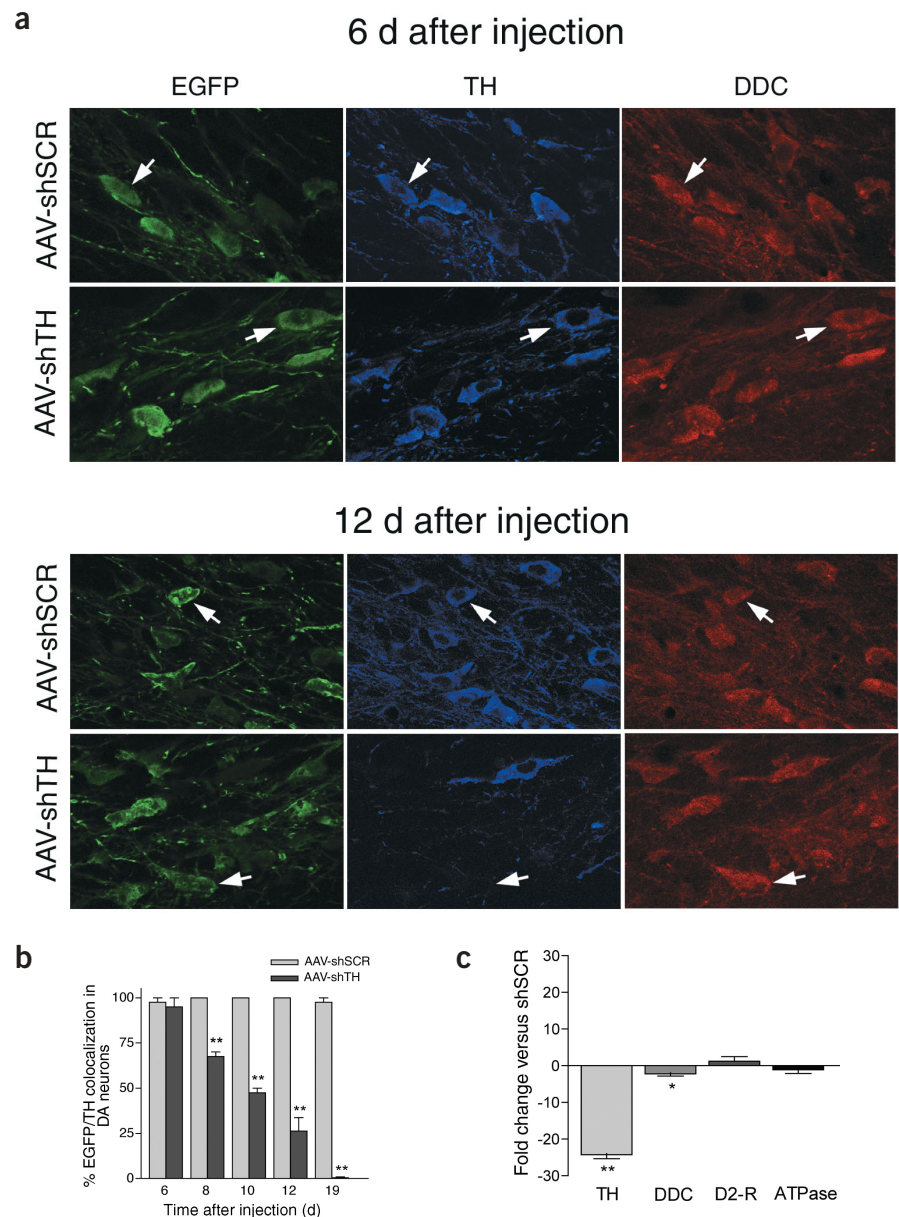


**Figure 1** Viral-mediated RNAi reduces tyrosine hydroxylase in the substantia nigra compacta. (a) Vector design to allow expression of a hairpin RNA that mediates RNAi, as well as an EGFP reporter to mark infected neurons. CMV, cytomegalovirus. (b,c) Fluorescent immunostaining for EGFP shows infected neurons from a 9-week-old mouse, taken 12 d after stereotaxic injection of AAV-shSCR on one side (b) and AAV-shTH on the other side (c) of the brain. (d,e) Fluorescent immunostaining for tyrosine hydroxylase (TH) in the substantia nigra compacta shows loss of tyrosine hydroxylase immunoreactivity in neurons infected with AAV-shTH (e) but not those infected with AAV-shSCR (d). (f,g) Merged image shows colocalization of EGFP and tyrosine hydroxylase in AAV-shSCR-infected neurons (f) but not in AAV-shTH-infected neurons (g). Magnification,  $\times 200$ .

**Figure 2** Time-course analysis of viral-mediated *Th* knockdown. Triple immunostaining for EGFP, tyrosine hydroxylase and DDC was used to characterize efficiency of *Th* knockdown. (a) No knockdown was visible 6 d after injection, but tyrosine hydroxylase was clearly lost from AAV-shTH-infected dopamine neurons by 12 d after injection. (b) Infected dopamine (DA) neurons were scored for tyrosine hydroxylase (TH) immunoreactivity ( $n = 2-4$  per time point). \*\*,  $P < 0.01$  by *t*-test. Magnification,  $\times 630$ . (c) Quantitative RT-PCR analysis of tyrosine hydroxylase, DDC, D2-R and vacuolar ATP synthase (ATPase) mRNA. \*,  $P < 0.05$ ; \*\*,  $P < 0.01$  by *t*-test;  $n = 3$  mice (two samples each done in duplicate).



by the infected neurons. Regions with high concentrations of EGFP-labeled axons showed a reduction in tyrosine hydroxylase, whereas regions innervated with AAV-shSCR-infected axons did not correlate with reduced tyrosine hydroxylase (Fig. 4c). This demonstrates the utility of the co-expressed EGFP marker for analysis of gene knockdown effects at relevant neuronal projection sites.

**Behavioral deficits in *Th* knockdown mice**

Finally, we found that RNAi-induced reduction in tyrosine hydroxylase can elicit behavioral defects. We first evaluated the effects of *Th* knockdown in the VTA on locomotor response to amphetamine, a well-established dopamine-dependent behavior<sup>23</sup>. Mice were given bilateral injections of either AAV-shTH or AAV-shSCR, and tested 16 d later when tyrosine hydroxylase expression was reduced (Figs. 1 and 2). After 4 d of saline injections, the mice were administered amphetamine (4 mg/kg), and locomotor activity was measured for 30 min. *Th* knockdown mice showed a significant ( $P < 0.01$ ) attenuation in locomotor response compared with controls, indicating that the viral-mediated gene knockdown was effective at modifying behavioral responses (Fig. 5a). Because dopamine function has been strongly implicated in motor control, we next evaluated rotarod performance in mice that received bilateral injections with AAV-shTH and AAV-shSCR in the substantia nigra compacta. After 17 d of infection, we evaluated rotarod performance twice a day for 3 d. As the mice continued training, those with a bilateral reduction in tyrosine hydroxylase showed a significant ( $P < 0.05$ ) deficit in rotarod performance (Fig. 5b). This phenotype is similar to neurotoxin-induced rodent models of Parkinson disease<sup>24,25</sup>, suggesting that attenuation of dopamine synthesis is sufficient to mimic motor deficiencies caused by neurodegeneration of the substantia nigra compacta. Notably, the average weights of the *Th* knockdown mice were not significantly different from those of control mice after targeting both the substantia nigra compacta (AAV-shTH mice, 26.2 g; AAV-shSCR mice, 25.5 g) and the VTA (AAV-shTH mice, 25.6 g;

AAV-shSCR mice, 24.9 g), suggesting that overall health was not affected by the gene knockdown.

**DISCUSSION**

This work shows the efficiency and power of RNAi for generating conditional mutations. We extend previous studies of RNAi in mammals<sup>12,13,26</sup> by using AAV to knock down endogenous gene expression in adult brain neurons and subsequently demonstrating a behavioral deficit. Moreover, we targeted specific brain regions and used an EGFP marker to conduct molecular analysis of both the modified neurons and their neuronal projection sites. This technique should facilitate future experiments to better define the relationship between genes, neural circuits and behavior.

The AAV-shRNA strategy provides practical advantages over existing techniques for the generation of conditional mutations. The creation of spatially restricted mutations using transgenic mice<sup>1</sup>, although powerful, has been challenging to control and

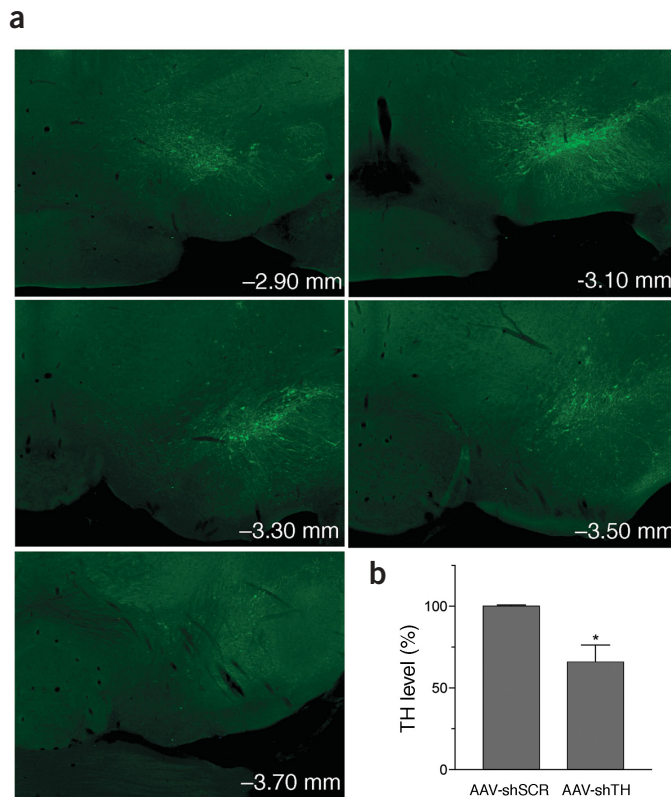


**Figure 3** AAV injection in the midbrain results in efficient infection of defined brain regions. **(a)** Low-power EGFP immunofluorescence shows ~800- $\mu$ m anterior-to-posterior spread of the virus, 12 d after injection into the substantia nigra compacta. Sections are arranged from anterior to posterior, with Bregma coordinates<sup>36</sup> listed in lower right corner. **(b)** Quantitative RT-PCR of laser-captured tissue shows 35% decrease in overall tyrosine hydroxylase (TH) in AAV-shTH-injected VTA.

function of tyrosine hydroxylase in mature mice and limited the genetic modification to specific regions of the midbrain. Mice with VTA-specific reductions in tyrosine hydroxylase showed an attenuated locomotor response to amphetamine, demonstrating the efficacy of RNAi-mediated gene knockdown. *Th* knockdown specific to the substantia nigra compacta produced a phenotype reminiscent of rodent models of Parkinson disease<sup>24,25</sup>, suggesting that loss of dopamine specifically in the adult substantia nigra compacta is sufficient to generate aberrant motor behavior. This approach should enable the testing of candidate genes for Parkinson disease<sup>31,32</sup> by altering their function specifically within the substantia nigra compacta.

Although modern microarray and proteomic strategies are resulting in the identification of many regulated genes and proteins, efficient *in vivo* tests of function will be needed to convert this data into a mechanistic understanding of systems biology. Somatic genetic manipulation using viral-mediated RNAi should facilitate this effort and accelerate the development of disease models. With AAV vectors, genetic disease models could be rapidly created in many species, including rodents and primates. The use of AAV in human clinical trials<sup>33</sup> presents the possibility that AAV-mediated RNAi could be used in gene therapy. The highly specific and sustained reduction of aberrant proteins by AAV may prove useful for treating a broad range of human diseases.

requires a significant investment of time and resources. In contrast, somatic genetic manipulation through RNAi allows us to rapidly create gene knockdowns in multiple brain regions. In addition, the strategy can be used on animals of different genetic backgrounds, including knockout and transgenic mice, and should also be effective in rats. The persistent expression of genes delivered by AAV allows animals to be evaluated for long-term effects of gene knockdown, and should provide stability to disease models. Moreover, modifications of AAV vector design will allow for inducible shRNA production<sup>27</sup>, simultaneous gene knockdowns<sup>28</sup> and cell-type-specific infection<sup>29</sup>.

Using viral-mediated gene knockdown, we have studied the role of tyrosine hydroxylase specifically in midbrain neurons. Mouse knockouts of *Th* are lethal<sup>30</sup>, and genetic removal of tyrosine hydroxylase from the dopamine system results in hypophagic mice that die at 3 weeks (ref. 20). In the present study, we reduced the

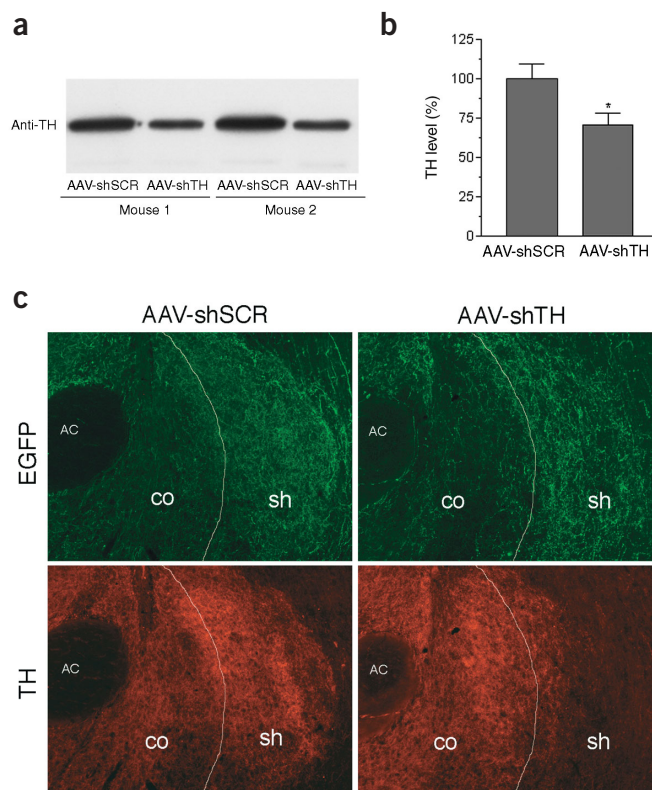


**Figure 4** Infection of VTA neurons reduces tyrosine hydroxylase in the nucleus accumbens. **(a)** Western blot analysis with antibody to tyrosine hydroxylase (anti-TH). Left and right nucleus accumbens extracts were examined from two representative mice injected with AAV-shTH and AAV-shSCR into either side of the VTA. **(b)** Quantitation of western blot data shows ~30% decrease in tyrosine hydroxylase in nucleus accumbens ( $n = 9$ ;  $P < 0.05$ ). **(c)** Regions of nucleus accumbens with high innervation by AAV-shTH-infected neurons showed reduction in tyrosine hydroxylase. White line demarcates approximate boundary between core (co) and shell (sh) of the nucleus accumbens and anterior commissure (AC). Top, infected neurons show prominent projections into the shell. Bottom, whereas regions of AAV-shTH projection correlate with those of decreased tyrosine hydroxylase staining (right panel), AAV-shSCR-infected side retains high levels of tyrosine hydroxylase (left panel).

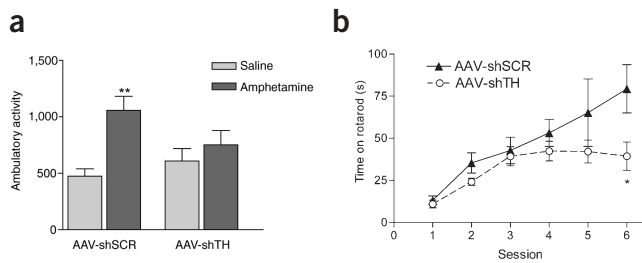


**Figure 5** Regional *Th* knockdown results in behavioral deficits. (a) VTA-specific knockdown mice do not show locomotor response to amphetamine, 16 d after bilateral injections of AAV-shTH and AAV-shSCR ( $n = 5$  for AAV-shTH;  $n = 8$  for AAV-shSCR; \*\*,  $P < 0.01$  by *t*-test). (b) *Th* knockdown in substantia nigra compacta reduces performance in rotarod test, 17 d after bilateral injections of AAV-shTH and AAV-shSCR. Average times are shown ( $n = 7$  for AAV-shTH;  $n = 6$  for AAV-shSCR; \*,  $P < 0.05$  by *t*-test).

## METHODS

**Mice.** We used 9- to 10-week-old male C57BL/6J mice (Jackson Laboratories). Mice were housed with 12-h light/dark cycles. All procedures were approved by the animal care committee at The University of Texas Southwestern Medical Center at Dallas.

**Design and construction of shRNA.** Hairpin RNA was designed to target specific regions of tyrosine hydroxylase mRNA<sup>10</sup>. We identified two 24-nucleotide stretches within the coding region of *Th* that were ~50% GC-rich, located within one exon, and unique in the genome. A random three-nucleotide loop structure, included with 24 nucleotides on either side of the loop, was designed to base-pair and form a hairpin. The hairpins were designed such that the antisense strand came before the sense strand during transcription. We synthesized three sets of oligonucleotides (Qiagen): shTH1 (top, 5'-TTTGAAGCTGATTGCATAGATTGCCTTCC-CAAGGCAATCTCTGCAATCAGCTTCTTTTT-3'; bottom, 5'-CTAGAAA AAGAAGCTGATTGCAGAGATTGCCTTGGGAAGGCAATCTATGCAA TCAGCTT-3'), shTH2 (top, 5'-TTTGGCTTACGGTGCAGGGCTGCT-GTCTTTGACAGCAGCCCTGCACCGCAAGCCTTTTT-3'; bottom, 5'-CTAGAAAAGGCTTGCAGGCTGCTGCTCAAAGACAGCAGCCCT-GCACCGTAAGC-3') and shSCR (top, 5'-TTTGTGGAGCCGAGTTTC-TAAATCCGCACCGGAATTTAGAAACCCGGCTCCACTTTTT-3'; bottom, 5'-CTAGAAAAGTGGAGCCGGTTTCTAAATCCGGTGCAGGAAATTA-GAAACTCGGCTCCA-3'). The oligonucleotides had *Bbs*I and *Xba*I overhangs to allow for ligation into the mU6pro plasmid<sup>10</sup>. All final clones were verified by sequencing. The mU6 promoter, hairpin sequence and terminator sequences were cut out using *Apa*I and *Kpn*I sites and ligated into a pAAV plasmid. The pAAV plasmid was designed to coexpress EGFP under the control of an independent RNA polymerase II promoter and terminator. This was done by removing EGFP from the pEGFP-N1 plasmid (Clontech) and ligating it first into pCMV-MCS (Stratagene), then into the pAAV plasmid using the *Acc*I and *Sma*I restriction sites.

**Viral production and purification.** Viral production was accomplished using a triple-transfection, helper-free method, and purified with a modified version of a published protocol<sup>34</sup>. Briefly, HEK 293 cells were cultured in ten 150 × 25 mm cell culture dishes and transfected with pAAV-shRNA, pHelper and pAAV-RC plasmids (Stratagene) using a standard calcium phosphate method. Cells were collected, pelleted and resuspended in freezing buffer (0.15 M NaCl and 50 mM Tris, pH 8.0) 66–70 h after transfection. After two freeze-thaw cycles to lyse the cells, benzoase was added (50 U/ml, final) and the mixture was incubated at 37 °C for 30 min. The lysate was added to a centrifuge tube containing a 15%, 25%, 40% and 60% iodixanol step gradient. The gradient was spun at 350,000 g for 60 min at 18 °C, and the 40% fraction was collected. This fraction was added to a heparin affinity column, washed with 0.1 M NaCl and eluted with 0.4 M NaCl. Elution buffer was exchanged with 1× PBS using Amicon BioMax

100K NMWL concentrators. The final purified virus was stored at –80 °C. The virus was then titered using an AAV ELISA kit (Progen) and used for infection of HT1080 cells.

**Stereotaxic surgery.** See Supplementary Methods online.

**Immunostaining.** Virus-injected mice were perfused and sectioned with standard protocols<sup>35</sup> (see Supplementary Methods online for details). Images in Figures 1 and 2 represent 4- $\mu$ m optical slices taken on a Zeiss 510 confocal microscope.

**Laser microdissection, RNA isolation and real-time PCR.** Brains were rapidly dissected out and frozen before sectioning. A Leica laser microdissection microscope (Leica LMD) was used to remove clusters of ~10–50 cells from 7- $\mu$ m sections taken on a cryostat and dehydrated in 75%, 95% and 100% ethanol for 20 s each. One region of the VTA containing AAV-shTH-infected neurons was captured; a region on the other side containing AAV-shSCR-infected neurons was captured as a control. RNeasy RNA purification columns (Qiagen) were used to purify RNA, followed by reverse transcription (First Strand Synthesis Kit, Invitrogen). Quantitative PCR was done in duplicate or triplicate using a Cepheid Smart-Cycler (1 cycle at 95 °C for 10 min; 44 cycles at 95 °C for 10 s, 58 °C for 5 s and 72 °C for 10 s; melt curve 58 °C–95 °C at 0.2 °C/s) with SYBR Green reaction mix (Roche Applied Science). GAPDH was used as a cDNA loading and PCR control. We used the following primers: tyrosine hydroxylase, 5'-CAGCC-CTACCAAGATCAAAC-3' and 5'-TACGGGTCAAACCTCACAGA-3'; GAP DH, 5'-AACGACCCCTTCATTGAC-3' and 5'-TCCACGACATACTCAGC AC-3'; D2-R, 5'-CAGATGCTTGCCATTGTTCT-3' and 5'-CAGCAGTGCA GGATCTTCAT-3'; vacuolar ATP synthase, 5'-ATCTGGCTAATGACCCA ACC-3' and 5'-GGCAGTTCATAGATTGTGG-3'; and DDC, 5'-TTCCG-GTATCTTCTGAATGG-3' and 5'-CCTGGTGACTGTGCTTTAGA-3'.

**Western blot analysis.** See Supplementary Methods online.

**Locomotor assay.** Sixteen days after bilateral injection of AAV-shTH or AAV-shSCR, intraperitoneal injections of saline were administered and locomotor activity was measured to establish a baseline. Amphetamine (4 mg/kg) was delivered intraperitoneally, and locomotor and ambulatory (successive beam-breaking) behavior was assessed for 30 min (San Diego Instruments).

**Rotarod.** Sixteen days after bilateral injection of AAV-shTH or AAV-shSCR, mice were tested over a 3-d period, with two sessions of five trials per day. Mice were allowed to rest for at least 60 min between each session. The rod (IITC Life Sciences) had a diameter of 3.8 cm and was accelerated from 0 to 30 r.p.m. over a 17.5-s period. Total time on the rotarod was measured. Time was stopped when mice fell from the rod or when they rotated around completely two times without walking (that is, holding on to the rod while rotating).

*Note: Supplementary information is available on the Nature Medicine website.*

## ACKNOWLEDGMENTS

We thank D. Turner for providing the U6 promoter-containing vector, L. Perrotti for rotarod assay protocols, E. Kim and L. Leverich for help with data collection, and C. Bolaños for advice on data analysis.

## COMPETING INTERESTS STATEMENT

The authors declare that they have no competing financial interests.

Received 9 July 2003; accepted 6 November 2003

Published online at <http://www.nature.com/naturemedicine/>

- Lewandoski, M. Conditional control of gene expression in the mouse. *Nat. Rev. Genet.* **2**, 743–755 (2001).
- Gossen, M. & Bujard, H. Studying gene function in eukaryotes by conditional gene inactivation. *Annu. Rev. Genet.* **36**, 153–173 (2002).
- DiLeone, R.J., Russell, L.B. & Kingsley, D.M. An extensive 3' regulatory region controls expression of *Bmp5* in specific anatomical structures of the mouse embryo. *Genetics* **148**, 401–408 (1998).
- Fire, A. *et al.* Potent and specific genetic interference by double-stranded RNA in

- Caenorhabditis elegans*. *Nature* **391**, 806–811 (1998).
5. Fraser, A.G. *et al.* Functional genomic analysis of *C. elegans* chromosome I by systematic RNA interference. *Nature* **408**, 325–330 (2000).
  6. Lum, L. *et al.* Identification of Hedgehog pathway components by RNAi in *Drosophila* cultured cells. *Science* **299**, 2039–2045 (2003).
  7. Kennerdell, J.R. & Carthew, R.W. Heritable gene silencing in *Drosophila* using double-stranded RNA. *Nat. Biotechnol.* **18**, 896–898 (2000).
  8. Kalidas, S. & Smith, D.P. Novel genomic cDNA hybrids produce effective RNA interference in adult *Drosophila*. *Neuron* **33**, 177–184 (2002).
  9. Elbashir, S.M. *et al.* Duplexes of 21-nucleotide RNAs mediate RNA interference in cultured mammalian cells. *Nature* **411**, 494–498 (2001).
  10. Yu, J.Y., DeRuiter, S.L. & Turner, D.L. RNA interference by expression of short-interfering RNAs and hairpin RNAs in mammalian cells. *Proc. Natl. Acad. Sci. USA* **99**, 6047–6052 (2002).
  11. Krichevsky, A.M. & Kosik, K.S. RNAi functions in cultured mammalian neurons. *Proc. Natl. Acad. Sci. USA* **99**, 11926–11929 (2002).
  12. McCaffrey, A.P. *et al.* RNA interference in adult mice. *Nature* **418**, 38–39 (2002).
  13. Xia, H., Mao, Q., Paulson, H.L. & Davidson, B.L. siRNA-mediated gene silencing *in vitro* and *in vivo*. *Nat. Biotechnol.* **20**, 1006–1010 (2002).
  14. McCown, T.J., Xiao, X., Li, J., Breese, G.R. & Samulski, R.J. Differential and persistent expression patterns of CNS gene transfer by an adeno-associated virus (AAV) vector. *Brain Res.* **713**, 99–107 (1996).
  15. Chamberlin, N.L., Du, B., de Lacalle, S. & Saper, C.B. Recombinant adeno-associated virus vector: use for transgene expression and anterograde tract tracing in the CNS. *Brain Res.* **793**, 169–175 (1998).
  16. McGeer, E.G., McGeer, P.L. & Wada, J.A. Distribution of tyrosine hydroxylase in human and animal brain. *J. Neurochem.* **18**, 1647–1658 (1971).
  17. Han, V.K., Snouweart, J., Towle, A.C., Lund, P.K. & Lauder, J.M. Cellular localization of tyrosine hydroxylase mRNA and its regulation in the rat adrenal medulla and brain by *in situ* hybridization with an oligodeoxyribonucleotide probe. *J. Neurosci. Res.* **17**, 11–18 (1987).
  18. Koob, G.F. & Nestler, E.J. The neurobiology of drug addiction. *J. Neuropsychiatry Clin. Neurosci.* **9**, 482–497 (1997).
  19. Berridge, K.C. & Robinson, T.E. What is the role of dopamine in reward: hedonic impact, reward learning, or incentive salience? *Brain Res. Brain Res. Rev.* **28**, 309–369 (1998).
  20. Zhou, Q.Y. & Palmiter, R.D. Dopamine-deficient mice are severely hypoactive, adipsic, and aphagic. *Cell* **83**, 1197–1209 (1995).
  21. Gibb, W.R. Functional neuropathology in Parkinson's disease. *Eur. Neurol.* **38** (suppl. 2), 21–50 (1997).
  22. Chuang, D., Zsilla, G. & Costa, E. Turnover rate of tyrosine hydroxylase during trans-synaptic induction. *Mol. Pharmacol.* **11**, 784–794 (1975).
  23. Moore, K.E. The actions of amphetamine on neurotransmitters: a brief review. *Biol. Psychiatry* **12**, 451–462 (1977).
  24. Colotla, V.A., Flores, E., Oscos, A., Meneses, A. & Tapia, R. Effects of MPTP on locomotor activity in mice. *Neurotoxicol. Teratol.* **12**, 405–407 (1990).
  25. Rozas, G., Lopez-Martin, E., Guerra, M.J. & Labandeira-Garcia, J.L. The overall rod performance test in the MPTP-treated-mouse model of Parkinsonism. *J. Neurosci. Methods* **83**, 165–175 (1998).
  26. Tiscornia, G., Singer, O., Ikawa, M. & Verma, I.M. A general method for gene knockdown in mice by using lentiviral vectors expressing small interfering RNA. *Proc. Natl. Acad. Sci. USA* **100**, 1844–1848 (2003).
  27. Fitzsimons, H.L., McKenzie, J.M. & Doring, M.J. Insulators coupled to a minimal bidirectional tet cassette for tight regulation of rAAV-mediated gene transfer in the mammalian brain. *Gene Ther.* **8**, 1675–1681 (2001).
  28. Yu, J.Y., Taylor, J., DeRuiter, S.L., Vojtek, A.B. & Turner, D.L. Simultaneous inhibition of GSK3 $\alpha$  and GSK3 $\beta$  using hairpin siRNA expression vectors. *Mol. Ther.* **7**, 228–236 (2003).
  29. Girod, A. *et al.* Genetic capsid modifications allow efficient re-targeting of adeno-associated virus type 2. *Nat. Med.* **5**, 1052–1056 (1999).
  30. Zhou, Q.Y., Quafe, C.J. & Palmiter, R.D. Targeted disruption of the tyrosine hydroxylase gene reveals that catecholamines are required for mouse fetal development. *Nature* **374**, 640–643 (1995).
  31. Polymeropoulos, M.H. *et al.* Mutation in the  $\alpha$ -synuclein gene identified in families with Parkinson's disease. *Science* **276**, 2045–2047 (1997).
  32. Kitada, T. *et al.* Mutations in the parkin gene cause autosomal recessive juvenile parkinsonism. *Nature* **392**, 605–608 (1998).
  33. Manno, C.S. *et al.* AAV-mediated factor IX gene transfer to skeletal muscle in patients with severe hemophilia B. *Blood* **101**, 2963–2972 (2003).
  34. Zolotukhin, S. *et al.* Recombinant adeno-associated virus purification using novel methods improves infectious titer and yield. *Gene Ther.* **6**, 973–985 (1999).
  35. Georgescu, D. *et al.* Involvement of the lateral hypothalamic peptide orexin in morphine dependence and withdrawal. *J. Neurosci.* **23**, 3106–3111 (2003).
  36. Paxinos, G. & Franklin, K.B.J. *The mouse brain in stereotaxic coordinates* (Academic Press, New York, 2000).